

GLOBAL SIMULATION OF UV ATMOSPHERIC EMISSIONS.

F. González-Galindo, M.A. López-Valverde, *Instituto de Astrofísica de Andalucía-CSIC, Granada, Spain.* (ggalindo@iaa.es), **F. Forget**, *Laboratoire de Météorologie Dynamique-IPSL, Paris, France*, **A. Stiepen, J.-C. Gérard**, *Laboratoire de Physique Atmosphérique et Planétaire, Space sciences, Technologies and Astrophysics Research Institute, University of Liege, Belgium*, **N.M. Schneider, S.K. Jain, J. Deighan**, *Laboratory for Atmospheric and Space Physics (LASP), University of Colorado, USA*, **J.-L. Bertaux**, *Laboratoire Atmospheres, Milieux, Observations Spatiales, IPSL, Paris, France.*

Introduction

UV atmospheric emissions arising from Mars were first observed by the Mariner missions (Barth et al., 1972; Stewart et al., 1972), and in more recent times by SPICAM on board Mars Express (Bertaux et al., 2005; Leblanc et al., 2006) and by IUVS on board MAVEN (Jain et al., 2015; Stiepen et al., 2016a). Some of the most prominent emissions in the dayside are the CO Cameron bands (wavelengths between about 190 and 260 nm) and the CO_2^+ UV doublet (289 nm). The nightside is dominated by the emission in the δ and γ bands of the NO emission system (190-270 nm). The study of these emissions provides important information about the interaction of the Martian atmosphere with the incoming solar radiation, the global circulation, or the density variability in the upper atmosphere.

Different models able to simulate these emissions have been developed to help interpreting the observations. A description of several of these models can be found in the introduction of Jain & Bhardwaj, 2012. Most of them are one-dimensional, i.e., only consider variations in the vertical direction. This allows for a very detailed treatment of the physical processes behind these atmospheric emissions without caring about the computational cost. On the other hand, these models often use a fixed background neutral atmosphere, or at best a few background atmospheres to take into account the seasonal and/or solar cycle variability, neglecting or reducing to a minimum the atmospheric variability. However, it is well known that the Martian upper atmosphere is very variable at different temporal and geographical scales (e.g. González-Galindo et al., 2015), and such a variability can affect some of the conclusions obtained by one-dimensional models.

We have included in the LMD Mars Global Climate Model (LMD-MGCM) a physical model of the Martian airglow able to simulate the CO Cameron bands, the CO_2^+ UV doublet and the NO nightglow. This model therefore provides a natural coupling between the UV airglow and the atmospheric variability. Our aims are to provide global maps of these atmospheric emission systems, to compare with observations whenever possible, to evaluate the effects of atmospheric variability over the predicted emissions, and to revisit some of the conclusions provided by previous one-dimensional models.

Physical processes

NO nightglow arises from the de-excitation of NO electronic states to its ground level. These excited molecules are formed by recombination of O and N atoms, which in turn are produced in the dayside thermosphere by photodissociation and by photoelectron impact dissociation of mainly CO_2 and N_2 , and later transported to the nightside. The excited state have a very short radiative lifetime, thus collisional de-excitation does not play an important role. This emission is a good tracer of the thermospheric dynamics transporting matter from the dayside to the nightside and from the summer to the winter hemisphere (e.g. Bertaux et al., 2005).

CO Cameron bands originate in the transition of the CO ($a^3\Pi$) excited state to the ground state. Different mechanisms populate the ($a^3\Pi$) state: photodissociation of CO_2 , photoelectron impact dissociation of CO_2 , photoelectron impact excitation of CO, dissociative recombination of CO_2^+ and fluorescence. 1D models have shown that the emission is dominated by the photoelectron impact dissociation of CO_2 below about 140 km and by the CO_2 photodissociation above, with minor contributions from the other processes (e.g. Shematovich et al., 2008; Jain & Bhardwaj, 2012). So, theoretically this emission could provide information about the CO_2 densities in the Martian upper atmosphere and the solar radiation-atmosphere interaction. However, the important uncertainties in the values of the different excitation cross sections usually prevents retrieval of CO_2 densities from this emission system (e.g. Gronoff et al., 2012). Atmospheric temperatures have been derived from the scale height of the emissions (Stiepen et al., 2015; Jain et al., 2015).

CO_2^+ UV doublet is produced by the de-excitation of the $\text{CO}_2^+(B^2\Sigma^+)$ state, which is populated by CO_2 photoionization and CO_2 photoelectron impact ionization. 1D calculations have shown that photoionization is the dominant process at all altitudes. This emission system has been used to retrieve CO_2 densities and temperatures in the upper atmosphere of Mars (Evans et al., 2015), and similarly to the CO Cameron band, temperature has also been derived from the emission scale height (Stiepen et al., 2015; Jain et al., 2015).

Implementation

The LMD-MGCM includes two different photochemical models. One of them (Lefevre et al., 2004) includes the complex chemical cycles important for the lower atmosphere, while the other one (González-Galindo et al., 2013) is particularly suited to the study of the rarified upper atmosphere, including the ionosphere. While the second one includes Nitrogen chemistry, the first one does not. The transition between both models is placed at the 0.1 Pa pressure level.

To simulate **NO nightglow**, the recombination of N and O atoms is traced in the upper atmosphere photochemical model. In our model, according to usual theoretical expectations, every recombination produces a photon in the NO emission system.

In order to simulate the **CO₂⁺ UV doublet** and the **Cameron bands**, several improvements were included with respect to the reference photochemistry. First, branching ratios to the different CO₂⁺ electronic states after CO₂ photoionization have been implemented. Second, a calculation of the energy with which the photoelectrons are created after photoionization has been included. Third, the degradation of the photoelectron energy when interacting with the atmosphere has been calculated following the Analytical Yield Spectrum (AYS) technique, based on detailed MonteCarlo calculations (Bhardwaj & Jain, 2009). Fourth, the excitation of the CO (*a*³Π) and the CO₂⁺ (*B*²Σ⁺) states from photoelectron impact has been incorporated by inclusion of the appropriate cross sections. And finally, a calculation of the volume emission rate (VER) from the different processes has been included. Then the predicted VERs are integrated along the line of sight using different observation geometries by means of a detailed raytracing calculation.

Results

The simulated zonal mean peak limb intensity of the **NO nightglow** at a constant local time LT=21, as a function of latitude and season, is shown in Fig. 1. This is similar to the map in Gagné et al., 2013. The white line is the 0.2 kR isoline, which corresponds approximately to the limit of detectability by the MAVEN/IUVS and the Mars Express/SPICAM instruments. The strongest emissions appear in the polar regions during the fall and winter seasons in each hemisphere. During the equinoxes some emissions, strong enough to be detected by SPICAM and IUVS, also appear in low and mid latitudes.

This global behavior is driven by the underlying variability of the general circulation. During equinoxes, meridional winds in the upper atmosphere are northward in the Northern hemisphere and southward in the Southern hemisphere, with vertical winds directed upwards in the low and mid latitudes and strong descending mo-

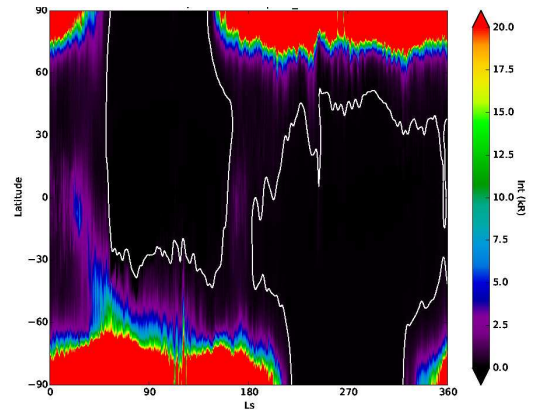


Figure 1: Zonal mean peak limb NO emission at LT=21 predicted by the LMD-MGCM

tions in the polar regions. This results in a transport of air from the low and mid latitudes of each hemisphere to its polar region, which tends to accumulate light species such as N and O in the poles. During solstices the situation is different. Focusing on the Southern summer case, meridional winds in the upper atmosphere are now northward at all latitudes, with vertical winds ascending in the summer hemisphere and descending over the winter hemisphere. This implies a transport of matter from the Southern (summer) hemisphere to the Northern (winter) pole, resulting in an accumulation of N and O in this region. The very weak emissions predicted by the model in the low and mid latitudes during solstice is related to a strong depletion in N (and not in O) at these latitudes with respect to the equinox case. The process(es) at the origin of this depletion is currently under investigation.

While average plots such as that in Fig. 1 are useful to show in a glance the most relevant aspects of the simulated emission, they neglect the longitudinal and local time variability. Fig. 2 shows the instantaneous NO VER predicted by the model at an altitude of 80 km from the surface, in a polar projection focused on the South pole of Mars, during the Ls=0-30 season. The morphology of the emission, which changes at every model's time step and which produces filaments that detach from the polar region and get to lower latitudes, produce a significant longitudinal and local time variability that needs to be taken into account when comparing with observations.

The comparison with MAVEN-IUVS observations is discussed in detail in Stiepen et al., 2016a, 2016b. In short, the altitude and intensity of the peak limb emission predicted by the model agree well with the observations during the equinox season (Ls=0-30). However, during the perihelion season (Ls=240-300), while our model reproduces the observed tendency of higher emission when approaching the polar winter, the model severely

UV ATMOSPHERIC EMISSIONS

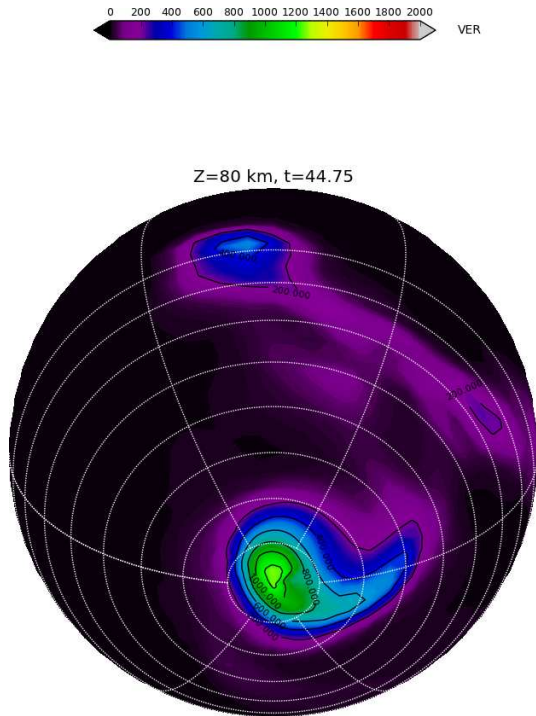


Figure 2: GCM simulation of the NO volume emission rate at an altitude of 80 km at $L_s=0$, around the South pole of Mars

underestimates by more than an order of magnitude the peak intensity and tends to overestimate the peak altitude in more than 10 km. Part of the differences in the peak altitude could be explained by our approximation of computing the thermospheric emission only above the 0.1 Pa level, as explained above. Moving the transition between both photochemical models in the LMD-MGCM to the 10 Pa level improves the comparison of the peak altitudes, but does not have a significant effect over the peak intensities.

Different possibilities have been explored to explain this underestimation of the emission in the mid latitudes of the northern (winter) hemisphere. One possibility is a model's underestimation of the production of N and O atoms. The model does not yet include the photoelectron impact dissociation, an important N source in the atmosphere of Venus (Gérard et al., 1988). However, the good agreement obtained in the equinox case suggests that there are not important production mechanisms lacking in the model. Another possibility is that the model is producing a too strong meridional transport, resulting in an excessive depletion of light species at low-mid latitudes and accumulation in the polar regions. Unfortunately, the observations at this season only cover a limited latitudinal range, preventing to confirm or dismiss this hypothesis. Finally, it is possible that the N chemistry is not well represented in the pho-

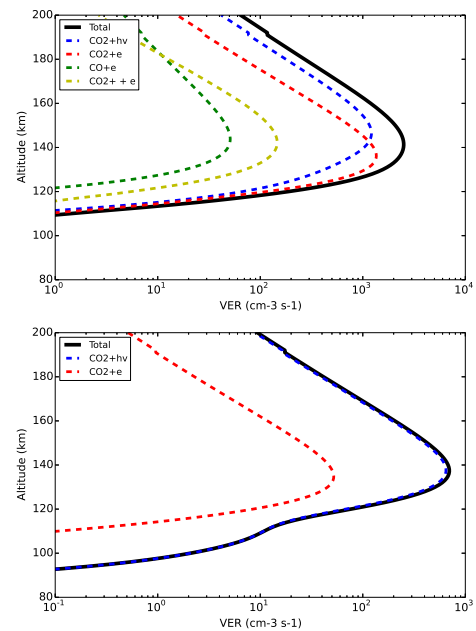


Figure 3: Volume emission rate of the CO Cameron bands (upper panel) and the CO_2^+ UV doublet, for conditions similar to those in Shematovich et al., 2008

tochemical model, producing the strong depletion of atomic nitrogen in the low and mid latitudes described above. We are currently exploring these possibilities.

MAVEN-IUVS has found a longitudinal variability of the NO emission during the northern winter season (Stiepen et al., 2016a, 2016b), with enhanced emission in a well-defined longitudinal range. Despite the differences in peak altitude and intensity with respect to the observations, the model predicts also enhanced intensity at the same longitudinal range. Which process can be producing this variability? A preliminary analysis of the predicted longitudinal and local time variability at this season shows disturbances moving with local time, which rules out the possibility of planetary standing waves. This preliminary analysis suggests a period of about 2 sols, which favors planetary travelling waves instead of non-migrating tides. A more detailed analysis, including a Fourier decomposition of the simulated variability, is needed for a more precise identification of the waves originating the predicted variability.

Regarding the **CO Cameron bands** and the **CO_2^+ UV doublet**, the global model is currently being tested and preliminary results will be discussed. Fig. 3 shows the vertical variability of the VER of both atmospheric emissions, and the contribution of the different processes populating the excited levels. The CO_2^+ UV doublet is

UV ATMOSPHERIC EMISSIONS

clearly dominated by CO₂ photoionization, while the Cameron bands is dominated by CO₂ photodissociation above about 140 km and by CO₂ electron impact dissociation below. Both the overall level of emission, the altitude of the peak emissions and the relative contribution of the different processes is in reasonable agreement with previous models (e.g. Shematovich et al., 2008, Jain & Bhardwaj, 2012).

Acknowledgements

This work has received funding from the European Union's Horizon 2020 Programme (H2020 - Compet - 08 - 2014) under grant agreement UPWARDS-633127. The Spanish team has been also supported by ESP2015-65064-C2-1-P (MINECO/FEDER)

References

- Barth, C. A., A. I. Stewart, C. W. Hord, and A. L. Lane (1972). Mariner 9 ultraviolet spectrometer experiment: Mars airglow spectroscopy and variations in Lyman alpha, *Icarus* 17, 457-468.
- Bertaux, J.-L., F. Leblanc, S. Perrier, et al. (2005). Nightglow in the upper atmosphere of Mars and implications for atmospheric transport, *Science*, vol. 307, 566-569.
- Bhardwaj, A., and S. K. Jain (2009). Monte Carlo model of electron energy degradation in a CO₂ atmosphere, *J. Geophys. Res.*, 114, A11309.
- Evans, J. S., M.H. Stevens, J.D. Lumpe, et al. (2015). Retrieval of CO₂ and N₂ in the Martian thermosphere using dayglow observations by IUVS on MAVEN, *Geophys. Res. Lett.*, 42.
- Gagné, M.-E., J.-L. Bertaux, F. González-Galindo, S. M. L. Melo, F. Montmessin, and K. Strong (2013). New nitric oxide (NO) nightglow measurements with SPICAM/MEx as a tracer of Mars upper atmosphere circulation and comparison with LMD-MGCM model prediction: Evidence for asymmetric hemispheres, *J. Geophys. Res. Planets*, 118, 2172-2179.
- Gérard, J. C., E. J. Deneye, and M. Lerho (1988). Sources and distribution of odd nitrogen in the Venus daytime thermosphere, *Icarus*, 75, 171-184.
- González-Galindo, F., J.-Y. Chaufray, M. A. López-Valverde, G. Gilli, F. Forget, F. Leblanc, R. Modolo, S. Hess, and M. Yagi (2013). Three-dimensional Martian ionosphere model: I. The photochemical ionosphere below 180 km, *J. Geophys. Res. Planets*, 118, 2105-2123.
- González-Galindo, F., M. A. López-Valverde, F. Forget, M. García-Comas, E. Millour, and L. Montabone (2015). Variability of the Martian thermosphere during eight Martian years as simulated by a ground-to-exosphere global circulation model, *J. Geophys. Res. Planets*, 120, 2020-2035.
- Gronoff, G., C. Simon Wedlund, C. J. Mertens, M. Barthélemy, R. J. Lillis, and O. Witasse (2012). Computing uncertainties in ionosphere-airglow models: II. The Martian airglow, *J. Geophys. Res.*, 117, A05309.
- Jain, S.K., and A. Bhardwaj (2012). Impact of solar EUV flux on CO Cameron band and CO₂⁺ UV doublet emissions in the dayglow of Mars, *Planet. and Space Sci.*, vol. 63-64, 110-122.
- Jain, S. K., A.I.F. Stewart, N.M. Schneider, et al. (2015). The structure and variability of Mars upper atmosphere as seen in MAVEN/IUVS dayglow observations, *Geophys. Res. Lett.*, 42.
- Leblanc, F., J. Y. Chaufray, J. Lilensten, O. Witasse, and J.-L. Bertaux (2006). Martian dayglow as seen by the SPICAM UV spectrograph on Mars Express, *J. Geophys. Res.*, 111, E09S11.
- Lefevre, F., S. Lebonnois, F. Montmessin, and F. Forget (2004). Three-dimensional modeling of ozone on Mars, *J. Geophys. Res.*, 109, E07004.
- Shematovich, V. I., D. V. Bisikalo, J.-C. Gérard, C. Cox, S. W. Bougher, and F. Leblanc (2008). Monte Carlo model of electron transport for the calculation of Mars dayglow emissions, *J. Geophys. Res.*, 113, E02011.
- Stewart, A. I., C. A. Barth, C. W. Hord, and A. L. Lane (1972). Mariner 9 ultraviolet spectrometer experiment: Structure of Mars's upper atmosphere, *Icarus* 17, 469-474.
- Stiepen, A., J.-C. Gérard, S. Bougher, F. Montmessin, B. Hubert, and J.-L. Bertaux (2015). Mars thermospheric scale height: CO Cameron and CO₂⁺ dayglow observations from Mars Express, *Icarus*, 245, 295-305.
- Stiepen, A., A.I.F. Stewart, S.K. Jain, et al. (2016a). Nitric Oxide Nightglow and inter-hemispheric transport at Mars mesosphere from MAVEN/IUVS observations, paper submitted.
- Stiepen, A., A.I.F. Stewart, S.K. Jain, et al. (2016b). Nitric Oxide Nightglow Mapping from IUVS Images and Implications for Seasonal Transport in Mars's Mesosphere, this issue.